diagnostics

MDPI

Review

Confocal Microscopy for Diagnosis and Management of Cutaneous Malignancies: Clinical Impacts and Innovation

Mehmet Fatih Atak [1], Banu Farabi [1], Cristian Navarrete-Dechent [2], Gennady Rubinstein [3], Milind Rajadhyaksha [4] and Manu Jain [4,5,*]

[1] Department of Dermatology, New York Medical College, Metropolitan Hospital, New York, NY 10029, USA
[2] Department of Dermatology, Escuela de Medicina, Pontificia Universidad Catolica de Chile, Santiago 8331150, Chile
[3] Dermatology and Laser Centre, Los Angeles, CA 91604, USA
[4] Dermatology Service, Department of Medicine, Memorial Sloan Kettering Cancer Center, New York, NY 10065, USA
[5] Dermatology Service, Department of Medicine, Weill Cornell Medicine, New York, NY 10021, USA
* Correspondence: jainm@mskcc.org; Tel.: +1-(646)-608-3562

Abstract: Cutaneous malignancies are common malignancies worldwide, with rising incidence. Most skin cancers, including melanoma, can be cured if diagnosed correctly at an early stage. Thus, millions of biopsies are performed annually, posing a major economic burden. Non-invasive skin imaging techniques can aid in early diagnosis and save unnecessary benign biopsies. In this review article, we will discuss in vivo and ex vivo confocal microscopy (CM) techniques that are currently being utilized in dermatology clinics for skin cancer diagnosis. We will discuss their current applications and clinical impact. Additionally, we will provide a comprehensive review of the advances in the field of CM, including multi-modal approaches, the integration of fluorescent targeted dyes, and the role of artificial intelligence for improved diagnosis and management.

Keywords: confocal microscopy; reflectance confocal microscopy; in vivo confocal microscopy; ex vivo confocal microscopy; innovations and advances in confocal microscopy in cutaneous oncology; clinical impacts in confocal microscopy in cutaneous oncology

Citation: Atak, M.F.; Farabi, B.; Navarrete-Dechent, C.; Rubinstein, G.; Rajadhyaksha, M.; Jain, M. Confocal Microscopy for Diagnosis and Management of Cutaneous Malignancies: Clinical Impacts and Innovation. *Diagnostics* **2023**, *13*, 854. https://doi.org/10.3390/diagnostics13050854

Academic Editors: Stamatia Giannarou and Cleopatra Charalampaki

Received: 28 December 2022
Revised: 10 February 2023
Accepted: 20 February 2023
Published: 23 February 2023

1. Introduction

Skin cancer is the most common cancer worldwide, with rising incidence [1]. The most common skin cancer is basal cell carcinoma (BCC), followed by squamous cell carcinoma (SCC), and melanoma [1–3]. Fortunately, when detected at an early stage, most skin cancers can be cured, including the deadliest cancer, melanoma [2,4]. Current diagnostic methods for detection of skin cancer are visual (naked eye) examination and dermoscopy. Although dermoscopy has improved the sensitivity for diagnosing skin cancers from 70.6% to 84.6% compared with visual examination alone, specificity of dermoscopy remains low (86%). This has resulted in a higher number needed to excise (NNE) of 5.23 with dermoscopy compared with visual evaluation alone (4.77), which leads to unnecessary biopsies of benign tissue [5].

Lower specificity of dermoscopic diagnosis is related to a lack of cellular resolution [6,7]. Thus, a biopsy is often performed for histopathological confirmation [8]. Biopsy is an invasive procedure that can be associated with complications such as bleeding, infection, delayed healing, and scars. Furthermore, a biopsy is a terminal procedure and does not allow to follow-up changes in a lesion over time. Although histopathology is the gold-standard, it cannot give an immediate bedside diagnosis due to time-consuming tissue processing, which may delay management and increase patients' anxiety. Moreover, the majority of the lesions biopsied to rule-out cancers are diagnosed as benign. Thus,

the overall diagnosis and management of skin cancer poses a heavy cost burden to public health and society at large [8–10].

To improve specificity and to detect skin cancers at earlier stages, non-invasive optical imaging techniques were developed in recent decades; confocal microscopy (CM) is one such technique. There are two types of CM: reflectance CM (RCM) and ex vivo CM (EVCM). Use of RCM can image skin lesions at a "quasi-histologic" level, in vivo, without need to perform a biopsy. Imaging relies solely on the reflectance contrast from various tissue components of the skin and does not use any exogenous contrast agent or dye (i.e., it is 'label free') [11]. The RCM device has acquired current procedural terminology (CPT) billing codes in the US and is primarily used to diagnose neoplastic and non-neoplastic skin lesions [12,13]. Lesions that are diagnosed benign on RCM are spared a biopsy (reducing unnecessary biopsies), while skin cancers, depending on their stage (early or late), proceed directly to treatment (surgical or nonsurgical). The use of RCM has also increased the accuracy of the non-invasive diagnosis of melanocytic [14] and non-melanocytic [15] skin cancers. For instance, the NNE for diagnosing melanoma has dropped to 3.0 with RCM (compared with 5.3 for dermoscopy alone) [7]. Moreover, RCM can be utilized for the surveillance of the recurrence of melanoma [16] or BCC [17], as well as the selection of appropriate treatment modalities for skin malignancies [18,19]. Importantly, reduced biopsy rates and the early detection of skin cancer have been shown to reduce the financial burden of skin cancer detection [10]. Although RCM has been shown to be valuable for the diagnosis and management of cutaneous tumors, there are certain limitations with the current commercial devices. These limitations are mostly due to the inherent nature of this technology, such as en-face visualization of the tissue, limited depth of imaging (~200 μm), small field of view (FOV) images (when using the handheld RCM device), grayscale images, and a lack of cellular specificity (i.e., the inability to differentiate dendritic melanocytes from Langerhans cells). Largely due to these difficulties with image interpretation and high cost, the adoption of RCM remains limited worldwide, despite its usefulness [20].

Unlike the RCM device, the EVCM device is used to image freshly excised tissues. While RCM imaging does not require dye application to the skin, EVCM imaging tissues are stained with a fluorescent nuclear dye. Thus, EVCM can be used to image tissues both in reflectance and fluorescence modes. The signals captured in these two modes are combined and can be digitally colored as purple-pink images (reflectance signal from collagen and cytoplasm in pink and fluorescent nuclear signal in purple), simulating hematoxylin and eosin (H&E)-stained histopathology [21]. This device is currently being integrated into Mohs surgery for the assessment of tumor margins [22]; however, it also can be used to evaluate skin lesions rapidly and as a potential adjunct tool to conventional histopathology evaluations. In particular, it could also be a valuable tool in resource-poor countries and remote areas where a histopathology laboratory set-up is not available.

In this review article, we will summarize the current evidence of both RCM and ECVM for their clinical impact on the diagnosis and management of skin cancers. Since the inception of CM, several innovations have occurred to improve the diagnostic accuracy of these devices and make them more user-friendly and widely available. These include: (1) building a combined RCM and optical coherence tomography (OCT) device (i.e., a multimodal approach), (2) the use of targeted molecular probes, (3) building cheaper and portable microscopes, and (4) integrating artificial intelligence (AI) algorithms to aid novices with image interpretation and diagnosis.

2. Current Application of Confocal Microscopy (CM)

2.1. Current Applications of Reflectance CM (RCM)

Features of skin cancers identifiable on RCM have been described in the literature [23–25]. The most common features of skin malignancies seen in RCM and their histopathologic correlates are summarized in Supplementary Table S1.

2.1.1. Skin Cancer Diagnosis and Management with RCM

Providing images at cellular resolution at the bedside in real time, RCM has been established as a valuable diagnostic tool for the detection of skin cancers, including melanocytic and keratinocyte cancers [26] (Figures 1A–C and S1A).

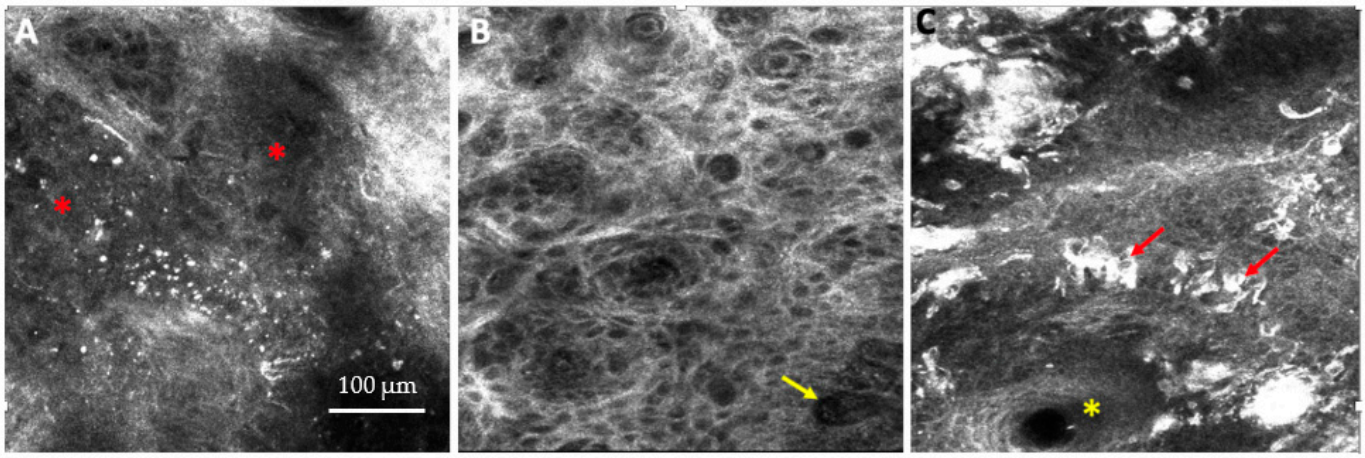

Figure 1. (**A**–**C**) Reflectance confocal microscopy (RCM) images of (**A**) basal cell carcinoma (BCC) showing tumor nodules (red asterisk), (**B**) squamous cell carcinoma showing an atypical honeycomb pattern at the spinosum layer with prominent vessels (yellow arrow), and (**C**) melanoma showing clusters of atypical melanocytes (red arrows) in the epidermis and around a hair follicle (yellow asterisk). Field of view: (**A**–**C**) = 500 × 500 µm. Image A courtesy of Ms. Rozina Zeidan, Clinical Research Specialist, Memorial Sloan Kettering Cancer Center.

Melanoma Diagnosis

Melanin has the highest refractive index, and therefore, appears bright on RCM, which makes it easy to visualize melanocytic lesions, including melanoma [26]. Dinnes et al. performed a test of diagnostic accuracy and showed that, at a fixed sensitivity of 90%, RCM's specificity was 82% for lesions clinically suspicious for melanoma and 86% for clinically equivocal lesions, compared with 42% and 49% on dermoscopy alone, respectively [14]. A subsequent meta-analysis conducted by Pezzini et al. reported similar results for the detection of melanoma via RCM, with a sensitivity of 92% (95% CI: 0.91–0.93) and a specificity of 70% (95% confidence interval [CI], 0.69–0.71). They also demonstrated that the use of RCM improves the accuracy of diagnosing melanoma compared with dermoscopy alone, achieving a sensitivity of 96% (95% CI, 0.93–0.98; I^2 = 75%) vs. 90% (95% CI, 0.86–0.93, I^2 = 0%), and specificity of 56% (95% CI, 0.52–0.60; I^2 = 97%) vs. 38% (95% CI, 0.34–0.42; I^2 = 98%), respectively [27]. In addition to its use in classic pigmented melanomas, RCM is also valuable for the diagnosis of amelanotic/hypomelanotic melanomas. In such cases, RCM has demonstrated a higher sensitivity of 67% (95% CI, 0.51–0.81) compared with 61% [95% CI, 0.37–0.81] for dermoscopy alone, with a similar specificity for both techniques (89% for RCM vs. 90% for dermoscopy alone) [28]. All of the aforementioned studies demonstrated that an increased diagnostic accuracy with RCM not only led to earlier detection of melanoma but has also reduced the rate of unnecessary benign excisions. To this end, a recent study by Pellacani et al. demonstrated that the use of RCM combined with dermoscopy reduces the NNE by 43.3% (from 5.3 to 3.0) in lesions suspected to be melanoma, as compared with the use of dermoscopy alone [7]. Furthermore, a cost–benefit analysis conducted in Italy showed that the routine use of RCM saved approximately EUR 260,000 per year per million inhabitants [10].

In addition to diagnosing melanoma in a new lesion, RCM shows promising results in detecting early melanoma changes in an existing lesion when used for a non-invasive imaging follow-up. Lesion monitoring performed with digital dermoscopy has a sensitivity

of 71.4% and a specificity of 63.4%, which could be increased to a 100% sensitivity with the addition of RCM [29].

In particular, RCM has been shown to be most useful for the diagnosis of melanomas located on the head and neck regions, on chronically sun-damaged skin, and for lesions with regression on dermoscopy. Lesions arising on the head and neck tend to be challenging due to the frequent presence of multiple freckles; solar lentigines; and flat, pigmented lesions that can mimic melanoma. Additionally, since it is a highly cosmetic and functional site, clinicians tend to avoid performing biopsies. RCM emerges as a valuable tool for the evaluation of lesions on these sites. Borsari et al. demonstrated that a higher diagnostic accuracy achieved through RCM significantly correlated with lesions located on sun damaged skin (Spearman analysis $\rho = 0.149$; $p < 0.001$) and lesions with dermoscopically observed regression ($\rho = 0.096$; $p = 0.001$) [30]. Lentigo maligna (LM) and its invasive counterpart LM melanoma (LMM) are the most common melanomas seen on chronically sun-damaged skin [31]. LMMs grow gradually during their horizontal (intraepidermal) growth phase and have a low mortality potential; however, they often mimic non-melanocytic neoplasms (pigmented actinic keratosis, seborrheic keratosis, solar lentigo, etc.), requiring biopsy for confirmation. To diagnose LM on the face within pigmented and non-pigmented equivocal lesions, diagnosticians have developed a scoring system based on RCM features; an LM score consists of two major features (nonedged papillae and pagetoid cells round and >20 mm in diameter, each scored two points) and three minor features (three or more atypical cells at the junction in five images, the follicular localization of pagetoid cells and/or atypical junctional cells, and nucleated cells within the papilla). An LM score of $\geq$2 on RCM has a sensitivity of 85% and specificity of 76% for the diagnosis of LM [32]. RCM may also be useful to discriminate LM from metal-induced cutaneous hyperpigmentation (e.g., tattoo, chrysiasis, argyriasis) [33].

RCM has a limited role in the diagnosis of nodular and acral melanomas. Although nodular melanomas can be visualized when located in the superficial dermis, deeper melanomas can be missed due to RCM imaging's limited depth of penetration (~250 µm) [20]. Likewise, acral sites have a thick stratum corneum which may hinder the visualization of melanoma due to high reflectance from the thick keratin layer [34]. Awareness of these limitations is crucial to prevent false negative diagnoses and subsequently devastating consequences.

Margin Assessment and Surveillance of Melanoma

LMs/LMMs are large ill-defined lesions with subclinical extensions that are challenging to detect visually and even with dermoscopy [35]. An inaccurate margin assessment often leads to incomplete excision of these lesions, increasing the risk of recurrence and additional surgery [36]. RCM is a highly valuable tool for the presurgical delineation of LM/LMM margins [37]. In these cases, the handheld RCM device [36] plays an important role, as it can be moved freely over the skin to map the lesion's extension. This device has shown a high sensitivity of 90% and a specificity of 86% for detecting these lesion types [37]. Guitera et al. reported that the use of RCM can identify the subclinical extension of LM 5 mm beyond the dermoscopically detected margin in 59% of patients [18]. The handheld device can also be used to guide biopsy acquisition in the most suspicious areas to assess invasion [38]. The device may also be used to select an appropriate treatment modality (i.e., surgical vs. non-surgical [radiotherapy or topical immunotherapy]) for treatment of these cancers [18]. This study also showed that, with the use of RCM, disease management strategies were changed in 73% of patients [18]. As compared with dermoscopy alone, the use of perioperative RCM was found to aide LM mapping during slow Mohs surgery and reduce the mean number of layers required for tumor clearance (from 1.54 layers to 1.29) and the mean time to repair (from 27 days to 14.6) ($p < 0.05$) [39].

Not only is RCM useful for margin assessments, but it can also be used to detect LM/LMM recurrence in scar tissue after surgical excision [16]. It is also useful for moni-

toring the response of unresectable melanomas to non-surgical therapies such as topical imiquimod, immunotherapy, and radiotherapy [40,41].

Basal Cell Carcinoma (BCC) Diagnosis and Management

RCM also plays an important role in the diagnosis and management of BCC, the most common skin cancer. There are several benign clinical mimics of BCC, most of which are present on the face. If diagnosed accurately in vivo, benign lesions can be spared biopsies, while BCCs can be triaged for a surgical or non-surgical approach (e.g., photodynamic therapy (PDT) or imiquimod for superficial and nodular lesions). A meta-analysis of 15 studies showed that RCM has a high pooled sensitivity and specificity of 92% (95% CI, 0.87–0.95; I^2 = 85.27%) and 93% (95% CI, 0.85–0.97; I^2 = 94.61%), respectively, for the diagnosis of BCC [42]. However, these studies did not specify the level of clinical difficulty in diagnosing these lesions, thus lacking evidence of RCM's utility for clinically challenging lesions. A randomized controlled multicenter trial compared RCM with punch biopsy for the diagnosis of BCC and demonstrated that RCM has a lower specificity (59.1% vs. 100.0%; $p < 0.001$), with a comparable sensitivity of 99.0% ($p = 1.0$) [43]. Additionally, the investigators demonstrated that RCM's sensitivity for the diagnosis of non-superficial BCC was not significantly different from that of punch biopsy (88.9% for RCM vs. 91.0% for biopsy; $p = 0.724$); furthermore, patient satisfaction was highly comparable for these two methods [43]. RCM is also valuable for the diagnosis and sub-typing of BCC and guidance of management (surgical vs. non-surgical), saving time, reducing cost, and improving comfort for patients [19,44].

The accuracy of diagnosing BCC on RCM has been compared with dermoscopy alone, especially for equivocal pink or lightly pigmented BCCs. Witkowski et al. demonstrated RCM's specificity to be slightly higher (93.8%) compared with dermoscopy alone (92.4%), though both had the same sensitivity (85.1%) [45]. A recent article by Dinnes et al. reported that, compared with dermoscopy, RCM demonstrated a higher sensitivity (94% vs. 85%), but a lower specificity (85% vs. 92%) [15].

Superficial BCC can be treated non-surgically when diagnosed early. This includes treatments such as topical therapies (e.g., 5% imiquimod, 5% fluorouracil) and destructive approaches (e.g., curettage, electrocautery, cryotherapy, laser ablation) [46]. Similar to its application for LM, RCM is also useful for monitoring response to non-invasive treatment of BCC. Guida et al. showed a pooled sensitivity of 100% and specificity of 72.5% for detecting persistent BCC after PDT or treatment with vismodegib [17].

RCM has been found to be effective in detecting residual BCC on clinically negative biopsy sites prior to Mohs surgery. Navarrete-Dechent et al. have shown a sensitivity of 92.8% and a specificity of 68.4% for the detection of residual BCC with RCM [47]. RCM has also been used intra-operatively to detect residual nonmelanoma skin cancers in lateral and deeper margins during Mohs surgery. In these cases, the use of RCM was able to detect residual tumors in 88% of lesions [48]. Similar results of 88.5% sensitivity and 91.7% specificity were reported with the use of RCM for the detection of BCC in wound margins [49]. Finally, RCM has been used to guide treatment with ablative lasers (such as CO_2 lasers) [19]; with such use, a total of 22% of cases required additional laser passes after real-time RCM evaluation of the treated site.

Squamous Cell Carcinoma (SCC) Diagnosis and Management

Similar to its use in the diagnosis of melanoma and BCC, RCM has been assessed for its efficacy for the diagnosis of SCC in equivocal lesions. A recent database meta-analysis demonstrated a sensitivity of 74–77% and a high specificity of 92–98% for the detection of SCC [15]. Another study showed a similar sensitivity of 74% (95% CI, 58–86%) and a specificity of 92% (95% CI, 88–95%) when the images were read by an experienced reader [50]. However, novices performed with a low sensitivity of 41%, but surprisingly, a higher specificity of 97% [50]. In contrast to its demonstrated value for diagnosis and

management of melanoma and BCC, more studies are needed to confirm the role of RCM for SCC.

2.2. Current Applications of Ex Vivo Confocal Microscopy (EVCM) in Dermatology

Using EVCM equipment (Figure 2A), physicians and expert readers have defined features of various skin lesions, including benign and malignant neoplasms (Figure 2B) and inflammatory lesions [51]. EVCM's major application is for the assessment of tumor margins during Mohs surgery. The device has shown a two-third reduction in time when compared with the requirements to process a frozen section ($p < 0.001$) [52].

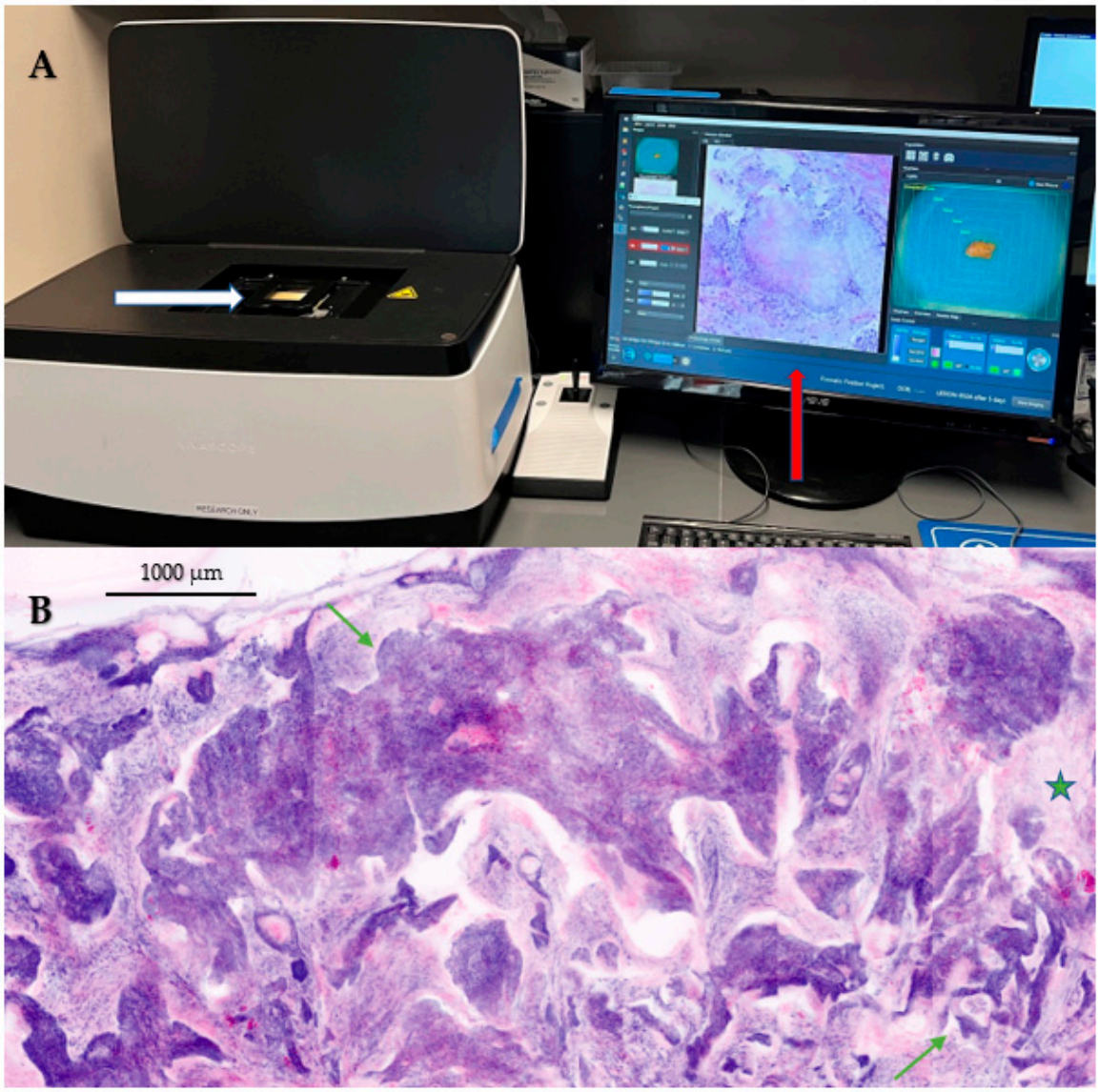

Figure 2. (**A**) An ex vivo confocal microscopy (EVCM) device with an attached computer screen for visualization of images in real-time. A fresh tissue from skin is mounted on a glass slide (white arrow) for imaging on the device and its digital hematoxylin and eosin (H&E) image (red arrow) is visible on the screen. (**B**) An EVCM image of a basal cell carcinoma in DHE mode showing nodular and infiltrative components (green arrows). Tumor nodules and cords appear purple due to fluorescent signals from nuclei, while stroma (green five-pointed star) appears pink due to reflectance signal, simulating H&E staining. Image A courtesy of Dr. Julia Kahn, Medical Graduate Student, Memorial Sloan Kettering Cancer Center.

2.2.1. EVCM for Diagnosis and Management of Melanoma

EVCM has been used to assess LM and LMM in surgical margins of 42 cutaneous and two mucosal LM/LMMs. The results for the diagnosis of cutaneous LM/LMM via EVCM were compared with those of in vivo RCM imaging [53]. The authors found that EVCM had a 95.5% rate of correct identification of tumor margins for both LM and LMM. This was comparable with the rate of 97.6% with cutaneous LM/LMM. Furthermore, EVCM demonstrated an ability to measure LM/LMM thickness in fresh tissues, which had a high correlation with the depth of tissue sections on histopathology; the mean difference was 0.09 ± 0.30 mm and 0.19 ± 0.35 mm on EVCM and histopathology. This study highlights the role of EVCM for perioperative decisions on safety margins for the excisions of LM/LMM in the future, potentially reducing time, cost, and the redundancy of processes [54].

2.2.2. EVCM for the Intra-Operative Margin Assessment of Keratinocyte Carcinomas

The use of EVCM has shown high sensitivity (79.8%) and specificity (95.8%) with a 95.7% negative predictive value for the detection of BCC in surgical margins during Mohs surgery [55]. Moreover, EVCM can be used to subtype residual BCCs reliably with a high diagnostic accuracy (90% for superficial BCC, 83% for nodular BCC, and 86% for infiltrative BCC) [56]. EVCM is also a useful tool to evaluate the surgical margin assessment of cutaneous SCC [22,57]. Horn et al. demonstrated that EVCM has an overall high sensitivity of 95% and specificity of 96.25% for the diagnosis of SCC in freshly excised skin lesions [58].

3. Advances in the Field of Confocal Microscopy (CM)

3.1. Enlarging the Field of View (FOV) of RCM Images

Although the arm-mounted RCM device can acquire images from a lesion measuring $\leq 8 \times 8$ mm, the FOV is smaller with the handheld device. To overcome this limitation, a video-mosaicking approach had been developed where "movies", i.e., live videos, are stitched together to provide a larger FOV. However, these videos often have motion-related artifacts due to rapid movements during image acquisition, thus affecting image quality. To reduce these artifacts, several AI algorithms have been built [59].

3.2. Multimodal Imaging

Various optical imaging devices have been combined with CM to overcome the limitations of CM, especially an en-face view of images, limited imaging depth, and a lack of cellular specificity. Such devices include RCM-OCT and RCM-multiphoton microscopy (MPM). Below, we describe some of these devices and their potential clinical applications.

3.2.1. RCM-Optical Coherence Tomography (OCT) Device

Recently, a combined RCM-OCT probe has been produced. OCT is another non-invasive optical imaging technique that has similar principles to ultrasound (US) imaging. While US imaging relies on the detection of signals generated by acoustic waves, OCT measures echo delays and the intensity of back-reflected infrared/near-infrared light [60]. Although the RCM device retrieves only a reflectance signal, the combination of OCT adds birefringence information from examined tissue. In RCM-OCT, both devices exist within a single handheld imaging probe and RCM and OCT images are co-registered [61] (Supplemental Figure S1B). While RCM provides high-resolution cellular-level information, OCT provides increased depth of imaging in a vertical mode, up to 1 mm (similar to histopathology) [61,62].

The combined probe has been explored primarily for the diagnosis and management of BCC (Figure 3A). In dermoscopically featureless, small ($\leq$1 cm), equivocal lesions, Monnier et al. demonstrated a 100% sensitivity and 100% specificity for detecting BCC, which is both superior to RCM alone (90% sensitivity, 62.5% specificity) and OCT alone (90% sensitivity, 50% specificity) [63]. Sahu et al. observed a correlation between histopathological depth and OCT-estimated depth, with a coefficient of determination (R2) of 0.75 ($R = 0.86$; $p < 0.001$) [64]. They conclude that this depth assessment can aid in the selection

of a treatment modality for BCC (i.e., surgical vs. non-surgical). In addition to the diagnosis of BCC, the use of RCM-OCT has been shown to be more effective in detecting residual BCC and delineating tumor margins than stand-alone RCM or OCT devices [61,65,66]. Aleissa et al. reported a sensitivity of 82.6% and a specificity of 93.8% for the detection of residual BCC in the surgical margin [67]. RCM-OCT has also served as an aid in the management of complex BCCs [66]. The use of a combined RCM-OCT probe may help by guiding treatment selection and defining the extent of surgery for BCCs.

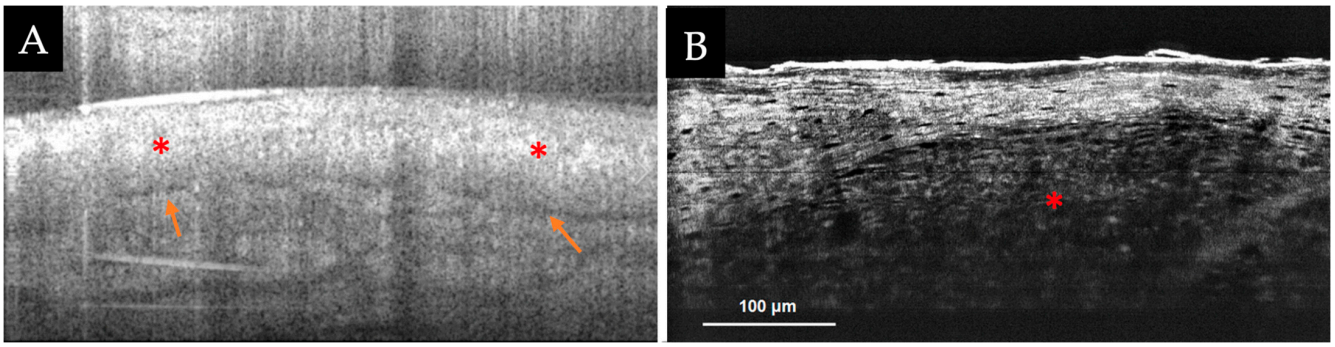

Figure 3. (**A**,**B**) Optical coherence tomography (OCT) images of tumor nodules (red asterisks) with clefting (orange arrows) from the BCC shown in Figure 1A acquired with (**A**, at left) an RCM-OCT probe, and (**B**, at right) high-resolution OCT device. Field of view: (**A**) = 2 × 1 mm; (**B**) = 500 × 400 µm. Images (**A**,**B**) courtesy of Ms. Rozina Zeidan, Clinical Research Specialist, Memorial Sloan Kettering Cancer Center.

Beyond its utility for BCC detection, this device has been explored for the diagnosis of other tumor types. Bang et al. showed potential for improving the detection of cutaneous metastases and differentiating them from vascular ectasia [68]. The authors described how RCM could detect tumor foci in the superficial dermis at a cellular resolution, while OCT aided in the detection of these foci in the deeper dermis. As cutaneous metastases also mimic primary cutaneous cancers, in future, this device could be also used to differentiate between these two entities.

3.2.2. High-Resolution Full-Field (FF)-OCT Devices

The recently developed FF-OCT device (Supplemental Figure S1C) uses a Gaussian-like broadband light source, which eliminates the artifact known as 'ghost image' and can provide ultra-high cellular resolution in B-scan mode (vertical mode), similar to conventional histopathological tissue sections. FF-OCT yields cross-sectional images with an axial resolution of 1.35 µm, lateral resolution of 1.3 µm, and scanning depth of 400 µm. Compared with the RCM device, the FOV for FF-OCT is smaller (~500 × 400 µm) [69]. Using FF-OCT, Wang et al. described the features of various neoplasms, including actinic keratosis, Bowen's disease, BCC, extramammary Paget's disease, seborrheic keratosis, and large cell acanthoma [70,71]. The team further evaluated the feasibility of FF-OCT for the diagnosis and subtyping of BCCs (Figure 3B). They reported that even a reader who was inexperienced (defined as a single 13 min training in FF-OCT) can use this technique to diagnose BCC with a sensitivity of 75% and a specificity of 57%, and subtype them with a sensitivity of 50% and a specificity of 57% [72].

3.2.3. Line Field (LC)-OCT

LC-OCT integrates the principle of OCT interferometry with the spatial filtering capabilities of RCM. This device provides high-resolution B-scan images in real time, with an isotropic spatial resolution of ~1 µm up to a depth of ~500 µm [73]. Compared with OCT, LC-OCT has a lower depth of penetration but superior resolution. Unlike RCM,

which can provide only horizontal images, LC-OCT generates both vertical and horizontal images at a similar cellular resolution as RCM [74].

Features of both non-melanocytic and melanocytic skin cancers have been defined using the LC-OCT device [75–78]. Compared with RCM, LC-OCT has been shown to yield a higher diagnostic accuracy for the detection of BCC. Ruini et al. demonstrated a 90.4% (95% CI, 79.0–96.8) agreement of LC-OCT with conventional histopathology in diagnosing BCC subtypes, which is superior to OCT (84%) and RCM (62.5%) [76]. The same authors also showed that the LC-OCT can improve dermatologists' confidence by 24.7% compared with clinical examination and dermoscopy [77] for the diagnosis of keratinocyte neoplasms (actinic keratosis, Bowen's disease, and invasive SCC). LC-OCT has been used non-invasively to predict the progression of an actinic keratosis to an invasive SCC, using a proliferation (PRO) grading system. This grading on LC-OCT had a 75% agreement with the grading on histopathology [79].

This device has also shown a higher accuracy for differentiating nevi from melanoma. Schuh et al. demonstrated that the use of LC-OCT yields superior diagnostic accuracy (97% overall accuracy, 93% sensitivity, 100% specificity) as compared with the use of RCM (94% overall accuracy, 93% sensitivity, 95% specificity) [75]. However, large-scale studies are required to validate these results.

3.2.4. Combined Multiphoton Microscopy (MPM)-RCM Device

Unlike RCM, which relies on the refractive index of various tissues, MPM is based on the nearly simultaneous absorption of two or more deeply penetrating near-infrared photons by endogenous fluorophores (keratin, melanin, etc.). Thus, it can be used to differentiate between various tissue structures. A combination of MPM with RCM enhances the capability to identify granules and minute particles of melanin and helps differentiate them from other morphologically similar fluorophores. Majdzadeh et al. accomplished the visualization of these melanin granules (both intracellular and extracellular) in the dermis and epidermis in a non-invasive manner even within non-lesional skin [80]. The utility of MPM-RCM in the detection of skin cancer remains understudied and warrants further exploration.

In addition to cell morphology, MPM can be used to quantify collagen patterns, especially collagen type 1, and can aid in the diagnosis and prognostication of cancer. Sendín et al. recently demonstrated that, solely based on the second harmonic signal obtained from collagen type 1, BCC can be distinguished from healthy skin. They could further subtype BCC as nonaggressive or aggressive [81]. The collagen-based information could be integrated with cellular details on MPM and RCM to improve the diagnosis and management of BCC.

3.3. Addition of Fluorescent Targeted Molecular Probes to Improve Diagnostic Accuracy of RCM

RCM imaging relies on the detection of singly backscattered light from sub-cellular structures. Melanin has the highest refractive index and appears bright, however, the nucleus has a weak backscatter from chromatin and appears dark [82]. This poses a major limitation in the visualization of tumors with a high nuclear-cytoplasmic ratio and increased nuclear density, such as BCC. To enhance the visualization of the nucleus, one may utilize exogenous molecule-targeted fluorescence nuclear contrast agents (e.g., poly (adenosine diphosphate-ribose), polymerase inhibitor-conjugated BODIPY-FL (PARPi-FL)) in combination with fluorescence (F)CM imaging. PARPi-FL has been shown to be overexpressed in BCC as compared with the surrounding normal adnexal structures (sebaceous gland, epidermis basal layer and hair follicle) and thus has the ability to provide a differential contrast. The use of PARPi-FL-labeled FCM imaging has the capability to improve the accuracy of diagnosis for BCC as compared with the use of reflectance (RCM) contrast alone; Sahu et al. demonstrated an improvement in sensitivity from 78.6–90% to 100% with slight or no improvement in specificity from 53.9% to 61.5% [83]. PARPi-FL dye is a small molecule that can penetrate intact skin via passive diffusion within 10–20 min

to reach the dermis and label BCC tumor nodules; as such, it has acquired the status of a new investigational drug for use in head and neck cancer. Thus, PARPi-FL has a promising potential for use during in vivo imaging of patients [83].

3.4. Enhancement of Tumor Detection via EVCM with Fluorescent-Labeled Antibodies

Although acridine orange, a nuclear dye, enhances the contrast between the nucleus and dermis, it is not a tumor-specific dye. Thus, tumor-specific fluorescent-labeled antibodies (such as S-100, Melan-A, and Ber-EP4) have been explored for the intraoperative diagnosis of skin tumors. Hartmann et al. reported the detection of S100 signal and Melan-A signal with EVCM imaging in 83.3% and 63.9% of metastatic melanoma tissue, while a Ber-EP4-positive fluorescent signal was detected in 83.30% of BCC tissues [84].

3.5. Dynamic Observation of Tumor Microenvironment (TME) to Predict the Response to Immunotherapy

TME comprises micro-vasculature, inflammatory cells, and mucin-surrounding tumors. TME is known to influence anti-tumor immunity and the response to immunotherapy treatment [85]. A change in TME can be used to predict the immunotherapy response; such changes can be evaluated on conventional histopathology tissue sections [86]. However, histopathology requires a biopsy, which is a terminal phenomenon and cannot be used to monitor lesions during a treatment course. Furthermore, only static images can be evaluated at a single site, which may result in the suboptimal prediction of the treatment response. Sahu et al. used in vivo RCM to observe dynamic TME features (tumor angiogenesis and leukocyte trafficking) to predict the response to immunotherapy. The investigators showed a correlation of TME features seen in melanoma and BCC on RCM as compared with the gold standard of histopathology. The authors also reported that the treatment response to imiquimod therapy in patients with BCC can be predicted by features of TME within RCM phenotypes (intra-tumoral inflammation, number of vessels or tumor-infiltrating lymphocytes, number of vessels) with 71% sensitivity and 83% specificity [87].

3.6. Building More Affordable and Portable Microscopes for Widespread Use

The currently available commercial CM devices (RCM and EVCM) are expensive, thus limiting their use in select large academic centers and in private clinics. Additionally, these devices are bulky and may not be practical for remote locations. In order to make CM devices more widely available across the world, manufacturers are producing more affordable and portable (smaller) versions of these devices [88,89]. For instance, to reduce the cost and complexity of conventional bulky RCM devices, a line-scanner RCM device has been developed. This device uses a single scanner and a linear-array detector that could drastically reduce the cost of this device to ~USD 15,000 [90].

A major innovation has been the development of a smartphone-attached-handheld-confocal microscope. These devices can visualize key cellular features of human skin in vivo with a comparable resolution to the commercially available confocal devices [91]. These portable devices are also inexpensive, as they use light-emitting diode (LED) as their light source and have an imaging sensor for capturing confocal images, instead of expensive lasers and bulky optoelectrical components (e.g., high-speed beam scanners, a fast data acquisition unit) used in the existing RCM devices [88,92]. This smartphone-based confocal microscope has been shown to have feasible use for the diagnosis of Kaposi's sarcoma in resource-limited settings in Uganda [89]. Despite their inexpensive nature and small footprint, these devices have some limitations. These include difficulty in maintaining stable contact between the device and skin, which may result in blurry images and a low signal-to-noise ratio (SNR) [88].

Furthermore, the commercial handheld RCM devices have been transformed into telescopic devices that can be used for imaging intra-oral lesions [93]. Peterson et al. used such a device to assess intra-operative margins of an oral SCC in awake patients. As this device has a small FOV image (0. 75 mm $\times$ 0.75 mm), the video-mosaicking approach

(Section 3.1) built for the commercial handheld device could be deployed to enable the visualization of a larger area (~4 mm × 2 mm) [94].

3.7. Integration of Artificial Intelligence (AI) Algorithms to Aid Novices with Confocal Microscopy Image Interpretation and Diagnosis

In addition to cost, another major limitation for the widespread use of these devices has been the inability of users to read confocal images. In vivo RCM images appear grayscale and in en-face view, thus requiring intensive training for novice readers to make correct diagnoses [12]. Although EVCM images are similar to H&E-stained ones, they may still require a trained pathologist or a Mohs surgeon for interpretation. AI or machine-learning-based approaches are widely integrated into various imaging modalities for the automated detection of cancers (such as lung cancers and lymph node metastases), including positron emission tomography (PET)/computed tomography (CT) [95]. Along a similar line, AI algorithms have been developed for both RCM and EVCM devices to overcome the limitations of image interpretation and aid novices in diagnosis [96–98].

3.7.1. AI for Diagnosis and Interpretation of In Vivo RCM Images

Wodzinski et al. developed an artificial neural network (ResNet) and demonstrated its accuracy to be 87% in classifying common skin neoplasms (melanoma, BCC, and nevi) using in vivo RCM images, an accuracy that was slightly better than human readers' ability [98]. Later, Campenella et al. developed a deep-learning-based AI model to automatically detect BCC in RCM images of clinically equivocal lesions. They showed that AI achieved a similar diagnostic accuracy as human expert readers with an area under the curve (AUC) for the receiver operator characteristic curve (ROC) of 89.7% (stack level) and 88.3% (lesion level). Their algorithm was also tested on an external dataset and demonstrated similar accuracy rates (AUC of 86.1%), indicating generalizability of the system's performance [99]. Machine learning can assist the clinician with pattern recognition in pigmented lesions. Soenen et al. showed that the machine learning can increase the diagnostic accuracy in the differentiation of congenital pigmented macules, such as café au lait spots, from congenital nevi on RCM images [100]. Kose et al. developed an automated semantic segmentation method called Multiscale Encoder-Decoder Network (MED-Net). They showed that MED-Net could achieve a pixel-wise mean sensitivity and specificity of 70 ± 11% and 95 ± 2%, respectively, for the detection of various patterns of melanocytic lesions at the dermal/epidermal junction (DEJ) in in vivo RCM images. Moreover, MED-Net successfully identified the location and extent of the pattern with 0.71 ± 0.09 Dice coefficient [101].

To overcome the limitation of grayscale images, Li et al. used a convolutional neural network to convert grayscale in vivo RCM images into virtually stained H&E-like images. They described this approach to visualize various normal skin layers (epidermis, DEJ, and superficial dermis), BCC, and nevi in a virtually stained H&E-like mode [102]. Such an approach could improve the interpretation of the RCM images due to readers' familiarity with the interpretation of H&E-stained images.

In addition to the above diagnostic algorithms, AI models have been built to aid technicians in image acquisition and to improve the quality of in vivo RCM images. Several artifacts (corneal layer reflection, shifting, and misalignment of mosaics related to patient movement, relicts occurring due to convexity of nodular lesions, air and oil bubbles, skin creases) may arise during image acquisition, impacting the quality of in vivo RCM images. AI helps clinicians to minimize these artifacts by using deep neural networks and other approaches [103]. Kose et al. showed that MED-Net could automatically detect artifacts in RCM images with 82% sensitivity and 93% specificity [104].

AI algorithms have been also developed for portable confocal devices; their main purpose is to improve the SNR ratio, which is crucial for attaining cellular-level resolution images. Zhao et al. tested a content-aware image restoration (CARE) approach, which is one of the deep-learning-based computational methods, to denoise images in high-speed

portable RCM to reduce SNR. With this approach, they achieved better noise reduction than the non-deep learning filtering methods yielded [105].

3.7.2. AI for EVCM Image Diagnosis and Interpretation

Similar to their use in in vivo RCM images, AI algorithms have been built to facilitate the reading of the EVCM images. Sendín-Martín et al. developed a deep-learning algorithm that achieved a 92% diagnostic accuracy for the automatic detection of BCC in EVCM images [97]. Later, Combalia et al. showed that their AI approach (U-Net architecture) could also detect BCC in EVCM images, with a sensitivity of 88% and specificity of 91% [96]. On EVCM images, Ruini et al. reported a high potential of deep learning models to detect cutaneous SCCs and to distinguish them from tumor-free skin, with an overall sensitivity of 76% and specificity of 91% [106].

Certain technical issues can impact the image quality of the EVCM images. One of the biggest issues is flattening the tissue on the glass slide during imaging, which leads to an incomplete visualization of the epidermis. This may impact the diagnosis of epidermal tumors such as superficial BCCs and SCCs. Sendín-Martín et al. built a three-dimensional mosaicking and intensity projection to overcome these limitations [107]. Furthermore, Combalia et al. also developed an AI model (U-Net architecture) to achieve virtual tissue flattening. They also developed a coloring algorithm to improve the appearance of the EVCM images [96].

3.8. Remote Reading of Confocal Images

Interpreting RCM images necessitates extensive training, typically requiring a couple of years. Thus, the accuracy of diagnosis on RCM is related to the reader's experience [12]. In order to integrate RCM imaging into clinical workflow, the novices need some assistance from an expert reader during imaging. As there is a paucity of expert readers worldwide, this limitation may be resolved via a telemedicine approach [50], which is now an integral part of dermatology and other medical fields.

As RCM images are digital in nature, they can be read remotely. Remote interpretation can be achieved via two methods: a standard store-and-forward (SAF) method [108,109] and a new live interactive method (LIM) tele-RCM [110]. With the SAF method, images are transferred to a remote expert reader after they are acquired, while with the LIM tele-RCM, the expert joins the imaging session with access to the screen in real-time. The SAF method reportedly showed an improved diagnostic accuracy with the addition of a second (expert reader) opinion [109,111]. On the other hand, the LIM tele-RCM method has several advantages compared with the SAF method, including an interaction between the clinician and expert reader and the ability to train novice readers and guide technicians to acquire diagnostic images. Rubinstein et al. demonstrated the feasibility of the LIM tele-RCM approach for the detection of a BCC [110]. This method could also be useful during pandemics, such as COVID-19, for remote reading. Large-scale studies are ongoing to assess its diagnostic accuracy in cutaneous malignancies.

Supplementary Materials: The following supporting information can be downloaded at: https://www.mdpi.com/article/10.3390/diagnostics13050854/s1, Figure S1: Photos of in vivo microscopes for used skin imaging; Table S1: Reflectance confocal microscopy (RCM) terms of the structures and their histopathological correlates in common skin malignancies.

Author Contributions: Reviewing literature, M.F.A., B.F., C.N.-D., M.R., G.R. and M.J.; Writing—original draft preparation M.F.A. and B.F.; writing—review and editing, M.F.A., B.F., C.N.-D., M.R., G.R. and M.J. All authors have read and agreed to the published version of the manuscript.

Funding: Research at Memorial Sloan Kettering Cancer Center is supported in part by the Memorial Sloan Kettering Cancer Center Support Grant/Core Grant (P30 CA008748) from the National Cancer Institute of the National Institutes of Health.

Data Availability Statement: Data sharing not applicable. No new data were created or analyzed in this study. Data sharing is not applicable to this article.

Acknowledgments: Limited editorial support at Memorial Sloan Kettering Cancer Center was provided by Katharine Olla Inoue, MA.

Conflicts of Interest: M.J. is a consultant for Enspectra Health, Inc.; the other authors (M.F.A., B.F., C.N.D., G.R., M.R.) declare no conflict of interest.

References

1. Urban, K.; Mehrmal, S.; Uppal, P.; Giesey, R.L.; Delost, G.R. The global burden of skin cancer: A longitudinal analysis from the Global Burden of Disease Study, 1990–2017. *JAAD Int.* **2021**, *2*, 98–108. [CrossRef] [PubMed]
2. Nikolaou, V.; Stratigos, A. Emerging trends in the epidemiology of melanoma. *Br. J. Dermatol.* **2014**, *170*, 11–19. [CrossRef]
3. Kwiatkowska, M.; Ahmed, S.; Ardern-Jones, M.; Bhatti, L.A.; Bleiker, T.O.; Gavin, A.; Hussain, S.; Huws, D.W.; Irvine, L.; Langan, S.M.; et al. An updated report on the incidence and epidemiological trends of keratinocyte cancers in the United Kingdom 2013–2018. *Ski. Health Dis.* **2021**, *1*, e61. [CrossRef]
4. Tripp, M.K.; Watson, M.; Balk, S.J.; Swetter, S.M.; Gershenwald, J.E. State of the science on prevention and screening to reduce melanoma incidence and mortality: The time is now. *CA Cancer J. Clin.* **2016**, *66*, 460–480. [CrossRef] [PubMed]
5. Hoorens, I.; Vossaert, K.; Lanssens, S.; Dierckxsens, L.; Argenziano, G.; Brochez, L. Value of Dermoscopy in a Population-Based Screening Sample by Dermatologists. *Dermatol. Pract. Concept.* **2019**, *9*, 200–206. [CrossRef]
6. Xiong, Y.-Q.; Ma, S.-J.; Mo, Y.; Huo, S.-T.; Wen, Y.-Q.; Chen, Q. Comparison of dermoscopy and reflectance confocal microscopy for the diagnosis of malignant skin tumours: A meta-analysis. *J. Cancer Res. Clin. Oncol.* **2017**, *143*, 1627–1635. [CrossRef] [PubMed]
7. Pellacani, G.; Farnetani, F.; Ciardo, S.; Chester, J.; Kaleci, S.; Mazzoni, L.; Bassoli, S.; Casari, A.; Pampena, R.; Mirra, M.; et al. Effect of Reflectance Confocal Microscopy for Suspect Lesions on Diagnostic Accuracy in Melanoma: A Randomized Clinical Trial. *JAMA Dermatol.* **2022**, *158*, 754–761. [CrossRef]
8. Terushkin, V.; Warycha, M.; Levy, M.; Kopf, A.W.; Cohen, D.E.; Polsky, D. Analysis of the Benign to Malignant Ratio of Lesions Biopsied by a General Dermatologist Before and After the Adoption of Dermoscopy. *Arch. Dermatol.* **2010**, *146*, 343–344. [CrossRef]
9. Tromme, I.; Legrand, C.; Devleesschauwer, B.; Leiter, U.; Suciu, S.; Eggermont, A.; Sacré, L.; Baurain, J.-F.; Thomas, L.; Beutels, P.; et al. Cost-effectiveness analysis in melanoma detection: A transition model applied to dermoscopy. *Eur. J. Cancer* **2016**, *67*, 38–45. [CrossRef]
10. Pellacani, G.; Witkowski, A.; Cesinaro, A.; Losi, A.; Colombo, G.; Campagna, A.; Longo, C.; Piana, S.; De Carvalho, N.; Giusti, F.; et al. Cost-benefit of reflectance confocal microscopy in the diagnostic performance of melanoma. *J. Eur. Acad. Dermatol. Venereol.* **2015**, *30*, 413–419. [CrossRef]
11. Longo, C.; Ragazzi, M.; Rajadhyaksha, M.; Nehal, K.; Bennassar, A.; Pellacani, G.; Guilera, J.M. In Vivo and Ex Vivo Confocal Microscopy for Dermatologic and Mohs Surgeons. *Dermatol. Clin.* **2016**, *34*, 497–504. [CrossRef] [PubMed]
12. Jain, M.; Pulijal, S.V.; Rajadhyaksha, M.; Halpern, A.C.; Gonzalez, S. Evaluation of Bedside Diagnostic Accuracy, Learning Curve, and Challenges for a Novice Reflectance Confocal Microscopy Reader for Skin Cancer Detection In Vivo. *JAMA Dermatol.* **2018**, *154*, 962–965. [CrossRef] [PubMed]
13. Yélamos, O.; Manubens, E.; Jain, M.; Chavez-Bourgeois, M.; Pulijal, S.V.; Dusza, S.W.; Marchetti, M.A.; Barreiro, A.; Marino, M.L.; Malvehy, J.; et al. Improvement of diagnostic confidence and management of equivocal skin lesions by integration of reflectance confocal microscopy in daily practice: Prospective study in 2 referral skin cancer centers. *J. Am. Acad. Dermatol.* **2020**, *83*, 1057–1063. [CrossRef] [PubMed]
14. Dinnes, J.; Deeks, J.J.; Saleh, D.; Chuchu, N.; Bayliss, S.E.; Patel, L.; Davenport, C.; Takwoingi, Y.; Godfrey, K.; Matin, R.N.; et al. Reflectance confocal microscopy for diagnosing cutaneous melanoma in adults. *Cochrane Database Syst. Rev.* **2018**, *12*, CD013190. [CrossRef] [PubMed]
15. Dinnes, J.; Deeks, J.J.; Chuchu, N.; Saleh, D.; E Bayliss, S.; Takwoingi, Y.; Davenport, C.; Patel, L.; Matin, R.N.; O'Sullivan, C.; et al. Reflectance confocal microscopy for diagnosing keratinocyte skin cancers in adults. *Cochrane Database Syst. Rev.* **2018**, *2018*, CD013191. [CrossRef] [PubMed]
16. Navarrete-Dechent, C.; Cordova, M.; Liopyris, K.; Rishpon, A.; Aleissa, S.; Rossi, A.; Lee, E.; Chen, C.; Busam, K.; Marghoob, A.; et al. Reflectance confocal microscopy and dermoscopy aid in evaluating repigmentation within or adjacent to lentigo maligna melanoma surgical scars. *J. Eur. Acad. Dermatol. Venereol.* **2020**, *34*, 74–81. [CrossRef] [PubMed]
17. Guida, S.; Alma, A.; Shaniko, K.; Chester, J.; Ciardo, S.; Proietti, I.; Giuffrida, R.; Zalaudek, I.; Manfredini, M.; Longo, C.; et al. Non-Melanoma Skin Cancer Clearance after Medical Treatment Detected with Noninvasive Skin Imaging: A Systematic Review and Meta-Analysis. *Cancers* **2022**, *14*, 2836. [CrossRef]
18. Guitera, P.; Moloney, F.J.; Menzies, S.W.; Stretch, J.R.; Quinn, M.J.; Hong, A.; Fogarty, G.; Scolyer, R.A. Improving Management and Patient Care in Lentigo Maligna by Mapping with In Vivo Confocal Microscopy. *JAMA Dermatol.* **2013**, *149*, 692–698. [CrossRef]
19. Navarrete-Dechent, C.; Cordova, M.; Liopyris, K.; Yélamos, O.; Aleissa, S.; Hibler, B.; Sierra, H.; Sahu, A.; Blank, N.; Rajadhyaksha, M.; et al. Reflectance confocal microscopy-guided carbon dioxide laser ablation of low-risk basal cell carcinomas: A prospective study. *J. Am. Acad. Dermatol.* **2019**, *81*, 984–988. [CrossRef]
20. Shahriari, N.; Grant-Kels, J.M.; Rabinovitz, H.; Oliviero, M.; Scope, A. Reflectance confocal microscopy: Principles, basic terminology, clinical indications, limitations, and practical considerations. *J. Am. Acad. Dermatol.* **2020**, *84*, 1–14. [CrossRef]

21. Malvehy, J.; Pérez-Anker, J.; Toll, A.; Pigem, R.; Garcia, A.; Alos, L.; Puig, S. Ex vivo confocal microscopy: Revolution in fast pathology in dermatology. *Br. J. Dermatol.* **2020**, *183*, 1011–1025. [CrossRef]
22. Longo, C.; Ragazzi, M.; Gardini, S.; Piana, S.; Moscarella, E.; Lallas, A.; Raucci, M.; Argenziano, G.; Pellacani, G. Ex vivo fluorescence confocal microscopy in conjunction with Mohs micrographic surgery for cutaneous squamous cell carcinoma. *J. Am. Acad. Dermatol.* **2015**, *73*, 321–322. [CrossRef]
23. Pellacani, G.; Scope, A.; Gonzalez, S.; Guitera, P.; Farnetani, F.; Malvehy, J.; Witkowski, A.; De Carvalho, N.; Lupi, O.; Longo, C. Reflectance confocal microscopy made easy: The 4 must-know key features for the diagnosis of melanoma and nonmelanoma skin cancers. *J. Am. Acad. Dermatol.* **2019**, *81*, 520–526. [CrossRef] [PubMed]
24. Navarrete-Dechent, C.; Liopyris, K.; Monnier, J.; Aleissa, S.; Boyce, L.M.; Longo, C.; Oliviero, M.; Rabinovitz, H.; Marghoob, A.A.; Halpern, A.C.; et al. Reflectance confocal microscopy terminology glossary for melanocytic skin lesions: A systematic review. *J. Am. Acad. Dermatol.* **2020**, *84*, 102–119. [CrossRef] [PubMed]
25. Navarrete-Dechent, C.; DeRosa, A.P.; Longo, C.; Liopyris, K.; Oliviero, M.; Rabinovitz, H.; Marghoob, A.A.; Halpern, A.C.; Pellacani, G.; Scope, A.; et al. Reflectance confocal microscopy terminology glossary for nonmelanocytic skin lesions: A systematic review. *J. Am. Acad. Dermatol.* **2018**, *80*, 1414–1427.e3. [CrossRef] [PubMed]
26. Shahriari, N.; Rabinovitz, H.; Oliviero, M.; Grant-Kels, J.M. Reflectance confocal microscopy: Melanocytic and nonmelanocytic. *Clin. Dermatol.* **2021**, *39*, 643–656. [CrossRef]
27. Pezzini, C.; Kaleci, S.; Chester, J.; Farnetani, F.; Longo, C.; Pellacani, G. Reflectance confocal microscopy diagnostic accuracy for malignant melanoma in different clinical settings: Systematic review and meta-analysis. *J. Eur. Acad. Dermatol. Venereol.* **2020**, *34*, 2268–2279. [CrossRef]
28. Lan, J.; Wen, J.; Cao, S.; Yin, T.; Jiang, B.; Lou, Y.; Zhu, J.; An, X.; Suo, H.; Li, D.; et al. The diagnostic accuracy of dermoscopy and reflectance confocal microscopy for amelanotic/hypomelanotic melanoma: A systematic review and meta-analysis. *Br. J. Dermatol.* **2020**, *183*, 210–219. [CrossRef] [PubMed]
29. Condorelli, A.G.; Farnetani, F.; Ciardo, S.; Chester, J.; Kaleci, S.; Stanganelli, I.; Mazzoni, L.; Magi, S.; Mandel, V.D.; Mirra, M.; et al. Dynamic dermoscopic and reflectance confocal microscopic changes of melanocytic lesions excised during follow up. *J. Am. Acad. Dermatol.* **2021**, *86*, 1049–1057. [CrossRef]
30. Borsari, S.; Pampena, R.; Lallas, A.; Kyrgidis, A.; Moscarella, E.; Benati, E.; Raucci, M.; Pellacani, G.; Zalaudek, I.; Argenziano, G.; et al. Clinical Indications for Use of Reflectance Confocal Microscopy for Skin Cancer Diagnosis. *JAMA Dermatol.* **2016**, *152*, 1093–1098. [CrossRef] [PubMed]
31. Matas-Nadal, C.; Malvehy, J.; Ferreres, J.R.; Boada, A.; Bodet, D.; Segura, S.; Salleras, M.; Azon, A.; Bel-Pla, S.; Bigata, X.; et al. Increasing incidence of lentigo maligna and lentigo maligna melanoma in Catalonia. *Int. J. Dermatol.* **2018**, *58*, 577–581. [CrossRef] [PubMed]
32. Guitera, P.; Pellacani, G.; Crotty, K.A.; Scolyer, R.A.; Li, L.-X.L.; Bassoli, S.; Vinceti, M.; Rabinovitz, H.; Longo, C.; Menzies, S.W. The Impact of In Vivo Reflectance Confocal Microscopy on the Diagnostic Accuracy of Lentigo Maligna and Equivocal Pigmented and Nonpigmented Macules of the Face. *J. Investig. Dermatol.* **2010**, *130*, 2080–2091. [CrossRef] [PubMed]
33. Martin, A.; Gouveia, B.M.; Rawson, R.; Guitera, P. Complex management of lentigo maligna in the setting of chrysiasis, argyriasis, and tattoo using in vivo reflectance confocal microscopy. *J. Dermatol.* **2022**, *49*, 703–709. [CrossRef] [PubMed]
34. Coco, V.; Farnetani, F.; Cesinaro, A.M.; Ciardo, S.; Argenziano, G.; Peris, K.; Pellacani, G.; Longo, C. False-Negative Cases on Confocal Microscopy Examination: A Retrospective Evaluation and Critical Reappraisal. *Dermatology* **2016**, *232*, 189–197. [CrossRef]
35. Zoutendijk, J.; Koljenovic, S.; Wakkee, M.; Mooyaart, A.; Nijsten, T.; Bos, R.V.D. Clinical findings are not helpful in detecting lentigo maligna melanoma in patients with biopsy-proven lentigo maligna. *J. Eur. Acad. Dermatol. Venereol.* **2022**, *36*, 2325–2330. [CrossRef]
36. Navarrete-Dechent, C.; Aleissa, S.; Cordova, M.; Liopyris, K.; Lee, E.H.; Rossi, A.M.; Hollman, T.; Pulitzer, M.; Lezcano, C.; Busam, K.J.; et al. Incompletely excised lentigo maligna melanoma is associated with unpredictable residual disease: Clinical features and the emerging role of reflectance confocal microscopy. *J. Eur. Acad. Dermatol. Venereol.* **2020**, *34*, 2280–2287. [CrossRef] [PubMed]
37. Elshot, Y.S.; Zupan-Kajcovski, B.; Klop, W.M.C.; Bekkenk, M.W.; Crijns, M.B.; Rie, M.A.; Balm, A.J.M. Handheld reflectance confocal microscopy: Personalized and accurate presurgical delineation of lentigo maligna (melanoma). *Head Neck* **2020**, *43*, 895–902. [CrossRef]
38. Hibler, B.P.; Yélamos, O.; Cordova, M.; Sierra, H.; Rajadhyaksha, M.; Nehal, K.S.; Rossi, A.M. Handheld reflectance confocal microscopy to aid in the management of complex facial lentigo maligna. *Cutis* **2017**, *99*, 346–352.
39. Gao, J.M.; Garioch, J.J.; Fadhil, M.; Tan, E.; Shah, N.; Moncrieff, M. Planning slow Mohs excision margins for lentigo maligna: A retrospective nonrandomized cohort study comparing reflectance confocal microscopy margin mapping vs. visual inspection with dermoscopy. *Br. J. Dermatol.* **2020**, *184*, 1182–1183. [CrossRef]
40. Navarrete-Dechent, C.; Cordova, M.; Aleissa, S.; Shoushtari, A.; Hollmann, T.J.; Leitao, M.M., Jr.; Rossi, A.M. Monitoring vulvar melanoma response to combined immunotherapy and radiotherapy with in vivo reflectance confocal microscopy. *Dtsch. Dermatol. Ges.* **2021**, *19*, 768–770. [CrossRef]
41. Ho, G.; Schwartz, R.; Pereira, A.R.; Dimitrou, F.; Paver, E.; McKenzie, C.; Saw, R.; Scolyer, R.; Long, G.; Guitera, P. Reflectance confocal microscopy—A non-invasive tool for monitoring systemic treatment response in stage III unresectable primary scalp melanoma. *J. Eur. Acad. Dermatol. Venereol.* **2022**, *36*, e583–e585. [CrossRef]

42. Lupu, M.; Popa, I.M.; Voiculescu, V.M.; Caruntu, A.; Caruntu, C. A Systematic Review and Meta-Analysis of the Accuracy of In Vivo Reflectance Confocal Microscopy for the Diagnosis of Primary Basal Cell Carcinoma. *J. Clin. Med.* **2019**, *8*, 1462. [CrossRef]
43. Woliner–van der Weg, W.; Peppelman, M.; Elshot, Y.S.; Visch, M.B.; Crijns, M.B.; Alkemade, H.A.C.; Bronkhorst, E.M.; Adang, E.; Amir, A.; Gerritsen, M.J.P.; et al. Biopsy outperforms reflectance confocal microscopy in diagnosing and subtyping basal cell carcinoma: Results and experiences from a randomized controlled multicentre trial*. *Br. J. Dermatol.* **2021**, *184*, 663–671. [CrossRef]
44. Kadouch, D.; Elshot, Y.; Zupan-Kajcovski, B.; van Haersma de With, A.S.E.; van der Wal, A.; Leeflang, M.; Jóźwiak, K.; Wolkerstorfer, A.; Bekkenk, M.; Spuls, P.; et al. One-stop-shop with confocal microscopy imaging vs. standard care for surgical treatment of basal cell carcinoma: An open-label, noninferiority, randomized controlled multicentre trial. *Br. J. Dermatol.* **2017**, *177*, 735–741. [CrossRef]
45. Witkowski, A.M.; Łudzik, J.; De Carvalho, N.T.; Ciardo, S.; Longo, C.; Dinardo, A.; Pellacani, G. Non-invasive diagnosis of pink basal cell carcinoma: How much can we rely on dermoscopy and reflectance confocal microscopy? *Ski. Res. Technol.* **2015**, *22*, 230–237. [CrossRef]
46. Peris, K.; Fargnoli, M.C.; Garbe, C.; Kaufmann, R.; Bastholt, L.; Seguin, N.B.; Bataille, V.; Marmol, V.D.; Dummer, R.; Harwood, C.A.; et al. Diagnosis and treatment of basal cell carcinoma: European consensus–based interdisciplinary guidelines. *Eur. J. Cancer* **2019**, *118*, 10–34. [CrossRef]
47. Navarrete-Dechent, C.; Cordova, M.; Aleissa, S.; Liopyris, K.; Dusza, S.W.; Phillips, W.; Rossi, A.M.; Lee, E.H.; Marghoob, A.A.; Nehal, K.S. Reflectance confocal microscopy confirms residual basal cell carcinoma on clinically negative biopsy sites before Mohs micrographic surgery: A prospective study. *J. Am. Acad. Dermatol.* **2019**, *81*, 417–426. [CrossRef]
48. Flores, E.S.; Córdova, M.; Kose, K.; Phillips, W.; Rossi, A.; Nehal, K.; Rajadhyaksha, M. Intraoperative imaging during Mohs surgery with reflectance confocal microscopy: Initial clinical experience. *J. Biomed. Opt.* **2015**, *20*, 61103. [CrossRef]
49. Shavlokhova, V.; Vollmer, M.; Vollmer, A.; Gholam, P.; Saravi, B.; Hoffmann, J.; Engel, M.; Elsner, J.; Neumeier, F.; Freudlsperger, C. In vivo reflectance confocal microscopy of wounds: Feasibility of intraoperative basal cell carcinoma margin assessment. *Ann. Transl. Med.* **2021**, *9*, 1716. [CrossRef]
50. Rao, B.K.; Mateus, R.; Wassef, C.; Pellacani, G. In vivo confocal microscopy in clinical practice: Comparison of bedside diagnostic accuracy of a trained physician and distant diagnosis of an expert reader. *J. Am. Acad. Dermatol.* **2013**, *69*, e295–e300. [CrossRef]
51. Vladimirova, G.; Ruini, C.; Kapp, F.; Kendziora, B.; Ergün, E.Z.; Bağcı, I.S.; Krammer, S.; Jastaneyah, J.; Sattler, E.C.; Flaig, M.J.; et al. Ex vivo confocal laser scanning microscopy: A diagnostic technique for easy real-time evaluation of benign and malignant skin tumours. *J. Biophotonics* **2022**, *15*, e202100372. [CrossRef]
52. Bennàssar, A.; Vilata, A.; Puig, S.; Malvehy, J. Ex vivo fluorescence confocal microscopy for fast evaluation of tumour margins during Mohs surgery. *Br. J. Dermatol.* **2014**, *170*, 360–365. [CrossRef]
53. Cinotti, E.; Belgrano, V.; Labeille, B.; Grivet, D.; Douchet, C.; Chauleur, C.; Cambazard, F.; Thomas, A.; Prade, V.; Tognetti, L.; et al. In vivo and ex vivo confocal microscopy for the evaluation of surgical margins of melanoma. *J. Biophotonics* **2020**, *13*, e202000179. [CrossRef]
54. Hartmann, D.; Krammer, S.; Ruini, C.; Ruzicka, T.; von Braunmühl, T. Correlation of histological and ex-vivo confocal tumor thickness in malignant melanoma. *Lasers Med. Sci.* **2016**, *31*, 921–927. [CrossRef]
55. Longo, C.; Pampena, R.; Bombonato, C.; Gardini, S.; Piana, S.; Mirra, M.; Raucci, M.; Kyrgidis, A.; Pellacani, G.; Ragazzi, M. Diagnostic accuracy of ex vivo fluorescence confocal microscopy in Mohs surgery of basal cell carcinomas: A prospective study on 753 margins. *Br. J. Dermatol.* **2019**, *180*, 1473–1480. [CrossRef]
56. Kose, K.; Fox, C.A.; Rossi, A.; Jain, M.; Cordova, M.; Dusza, S.W.; Ragazzi, M.; Gardini, S.; Moscarella, E.; Diaz, A.; et al. An international 3-center training and reading study to assess basal cell carcinoma surgical margins with ex vivo fluorescence confocal microscopy. *J. Cutan. Pathol.* **2021**, *48*, 1010–1019. [CrossRef]
57. Grizzetti, L.; Kuonen, F. Ex vivo confocal microscopy for surgical margin assessment: A histology-compared study on 109 specimens. *Ski. Health Dis.* **2022**, *2*, e91. [CrossRef]
58. Horn, M.; Gerger, A.; Koller, S.; Weger, W.; Langsenlehner, U.; Krippl, P.; Kerl, H.; Samonigg, H.; Smolle, J. The use of confocal laser-scanning microscopy in microsurgery for invasive squamous cell carcinoma. *Br. J. Dermatol.* **2007**, *156*, 81–84. [CrossRef]
59. Kose, K.; Gou, M.; Yélamos, O.; Cordova, M.; Rossi, A.M.; Nehal, K.S.; Flores, E.S.; Camps, O.; Dy, J.G.; Brooks, D.H.; et al. Automated video-mosaicking approach for confocal microscopic imaging in vivo: An approach to address challenges in imaging living tissue and extend field of view. *Sci. Rep.* **2017**, *7*, 10759. [CrossRef]
60. Gambichler, T.; Jaedicke, V.; Terras, S. Optical coherence tomography in dermatology: Technical and clinical aspects. *Arch. Dermatol. Res.* **2011**, *303*, 457–473. [CrossRef]
61. Harris, U.; Rajadhyaksha, M.; Jain, M. Combining Reflectance Confocal Microscopy with Optical Coherence Tomography for Noninvasive Diagnosis of Skin Cancers via Image Acquisition. *J. Vis. Exp.* **2022**, 186. [CrossRef]
62. Jung, J.M.; Cho, J.Y.; Lee, W.J.; Chang, S.E.; Lee, M.W.; Won, C.H. Emerging Minimally Invasive Technologies for the Detection of Skin Cancer. *J. Pers. Med.* **2021**, *11*, 951. [CrossRef]
63. Monnier, J.; De Carvalho, N.; Harris, U.; Garfinkel, J.; Saud, A.; Navarrete-Dechent, C.; Liopyris, K.; Reiter, O.; Rubinstien, G.; Iftimia, N.; et al. Combined reflectance confocal microscopy and optical coherence tomography to improve the diagnosis of equivocal lesions for basal cell carcinoma. *J. Am. Acad. Dermatol.* **2021**, *86*, 934–936. [CrossRef]

64. Sahu, A.; Yélamos, O.; Iftimia, N.; Cordova, M.; Alessi-Fox, C.; Gill, M.; Maguluri, G.; Dusza, S.W.; Navarrete-Dechent, C.; Gonzalez, S.; et al. Evaluation of a Combined Reflectance Confocal Microscopy–Optical Coherence Tomography Device for Detection and Depth Assessment of Basal Cell Carcinoma. *JAMA Dermatol.* **2018**, *154*, 1175–1183. [CrossRef]
65. Iftimia, N.; Yélamos, O.; Chen, C.-S.J.; Maguluri, G.; Cordova, M.A.; Sahu, A.; Park, J.; Fox, W.; Alessi-Fox, C.; Rajadhyaksha, M. Handheld optical coherence tomography–reflectance confocal microscopy probe for detection of basal cell carcinoma and delineation of margins. *J. Biomed. Opt.* **2017**, *22*, 76006. [CrossRef]
66. Navarrete-Dechent, C.; Aleissa, S.; Cordova, M.; Liopyris, K.; Sahu, A.; Rossi, A.M.; Lee, E.H.; Nehal, K.S. Management of complex head-and-neck basal cell carcinomas using a combined reflectance confocal microscopy/optical coherence tomography: A descriptive study. *Arch. Dermatol. Res.* **2020**, *313*, 193–200. [CrossRef]
67. Aleissa, S.; Navarrete-Dechent, C.; Cordova, M.; Sahu, A.; Dusza, S.W.; Phillips, W.; Rossi, A.; Lee, E.; Nehal, K.S. Presurgical evaluation of basal cell carcinoma using combined reflectance confocal microscopy–optical coherence tomography: A prospective study. *J. Am. Acad. Dermatol.* **2020**, *82*, 962–968. [CrossRef]
68. Bang, A.; Monnier, J.; Harris, U.; Garfinkel, J.; Rubinstein, G.; Iftimia, N.; Pulitzer, M.; Murray, M.; Lacouture, M.; Jain, M. Non-invasive, in vivo, characterization of cutaneous metastases using a novel multimodal RCM-OCT imaging device: A case-series. *J. Eur. Acad. Dermatol. Venereol.* **2022**, *36*, 2051–2054. [CrossRef]
69. Ho, T.-S.; Tsai, M.-R.; Lu, C.-W. In vivo Mirau-type optical coherence microscopy with symmetrical illumination. In *Optical Coherence Tomography and Coherence Domain Optical Methods in Biomedicine XXIV*; SPIE: Bellingham, WA, USA, 2020; Volume 11228.
70. Wang, Y.-J.; Wang, J.-Y.; Wu, Y.-H. Application of Cellular Resolution Full-Field Optical Coherence Tomography in vivo for the Diagnosis of Skin Tumours and Inflammatory Skin Diseases: A Pilot Study. *Dermatology* **2022**, *238*, 121–131. [CrossRef]
71. Wang, J.; Wang, Y.; Wu, Y. In vivo characterization of extramammary Paget's disease by ultra-high cellular resolution optical coherence tomography. *Ski. Res. Technol.* **2020**, *27*, 114–117. [CrossRef]
72. Wang, Y.; Chang, W.; Wang, J.; Wu, Y. Ex vivo full-field cellular-resolution optical coherence tomography of basal cell carcinomas: A pilot study of quality and feasibility of images and diagnostic accuracy in subtypes. *Ski. Res. Technol.* **2020**, *26*, 308–316. [CrossRef]
73. Dubois, A.; Levecq, O.; Azimani, H.; Siret, D.; Barut, A.; Suppa, M.; Del Marmol, V.; Malvehy, J.; Cinotti, E.; Rubegni, P.; et al. Line-field confocal optical coherence tomography for high-resolution noninvasive imaging of skin tumors. *J. Biomed. Opt.* **2018**, *23*, 106007. [CrossRef]
74. Ruini, C.; Schuh, S.; Sattler, E.; Welzel, J. Line-field confocal optical coherence tomography—Practical applications in dermatology and comparison with established imaging methods. *Ski. Res. Technol.* **2021**, *27*, 340–352. [CrossRef]
75. Schuh, S.; Ruini, C.; Perwein, M.K.E.; Daxenberger, F.; Gust, C.; Sattler, E.C.; Welzel, J. Line-Field Confocal Optical Coherence Tomography: A New Tool for the Differentiation between Nevi and Melanomas? *Cancers* **2022**, *14*, 1140. [CrossRef]
76. Ruini, C.; Schuh, S.; Gust, C.; Kendziora, B.; Frommherz, L.; French, L.E.; Hartmann, D.; Welzel, J.; Sattler, E. Line-field optical coherence tomography: In vivo diagnosis of basal cell carcinoma subtypes compared with histopathology. *Clin. Exp. Dermatol.* **2021**, *46*, 1471–1481. [CrossRef]
77. Ruini, C.; Schuh, S.; Gust, C.; Kendziora, B.; Frommherz, L.; French, L.E.; Hartmann, D.; Welzel, J.; Sattler, E.C. Line-field confocal optical coherence tomography for the in vivo real-time diagnosis of different stages of keratinocyte skin cancer: A preliminary study. *J. Eur. Acad. Dermatol. Venereol.* **2021**, *35*, 2388–2397. [CrossRef]
78. Cinotti, E.; Tognetti, L.; Cartocci, A.; Lamberti, A.; Gherbassi, S.; Cano, C.O.; Lenoir, C.; Dejonckheere, G.; Diet, G.; Fontaine, M.; et al. Line-field confocal optical coherence tomography for actinic keratosis and squamous cell carcinoma: A descriptive study. *Clin. Exp. Dermatol.* **2021**, *46*, 1530–1541. [CrossRef]
79. Ruini, C.; Schuh, S.; Gust, C.; Hartmann, D.; French, L.; Sattler, E.; Welzel, J. In-Vivo LC-OCT Evaluation of the Downward Proliferation Pattern of Keratinocytes in Actinic Keratosis in Comparison with Histology: First Impressions from a Pilot Study. *Cancers* **2021**, *13*, 2856. [CrossRef]
80. Majdzadeh, A.; Lee, A.M.D.; Wang, H.; Lui, H.; McLean, D.I.; Crawford, R.I.; Zloty, D.; Zeng, H. Real-time visualization of melanin granules in normal human skin using combined multiphoton and reflectance confocal microscopy. *Photodermatol. Photoimmunol. Photomed.* **2015**, *31*, 141–148. [CrossRef]
81. Sendín-Martín, M.; Posner, J.; Harris, U.; Moronta, M.; Sánchez, J.C.; Mukherjee, S.; Rajadhyaksha, M.; Kose, K.; Jain, M. Quantitative collagen analysis using second harmonic generation images for the detection of basal cell carcinoma with ex vivo multiphoton microscopy. *Exp. Dermatol.* **2022**. [CrossRef]
82. Rajadhyaksha, M.; Gonzalez, S.; Zavislan, J.M. Detectability of contrast agents for confocal reflectance imaging of skin and microcirculation. *J. Biomed. Opt.* **2004**, *9*, 323–331. [CrossRef]
83. Sahu, A.; Cordero, J.; Wu, X.; Kossatz, S.; Harris, U.; Franca, P.D.D.; Kurtansky, N.R.; Everett, N.; Dusza, S.; Monnier, J.; et al. Combined PARP1-Targeted Nuclear Contrast and Reflectance Contrast Enhance Confocal Microscopic Detection of Basal Cell Carcinoma. *J. Nucl. Med.* **2022**, *63*, 912–918. [CrossRef] [PubMed]
84. Hartmann, D.; Krammer, S.; Vural, S.; Bachmann, M.R.; Ruini, C.; Sárdy, M.; Ruzicka, T.; Berking, C.; Von Braunmühl, T. Immunofluorescence and confocal microscopy for ex-vivo diagnosis of melanocytic and non-melanocytic skin tumors: A pilot study. *J. Biophotonics* **2018**, *11*, e201700211. [CrossRef] [PubMed]
85. Tang, T.; Huang, X.; Zhang, G.; Hong, Z.; Bai, X.; Liang, T. Advantages of targeting the tumor immune microenvironment over blocking immune checkpoint in cancer immunotherapy. *Signal Transduct. Target. Ther.* **2021**, *6*, 72. [CrossRef]

86. Galon, J.; Bruni, D. Approaches to treat immune hot, altered and cold tumours with combination immunotherapies. *Nat. Rev. Drug Discov.* **2019**, *18*, 197–218. [CrossRef] [PubMed]
87. Sahu, A.; Kose, K.; Kraehenbuehl, L.; Byers, C.; Holland, A.; Tembo, T.; Santella, A.; Alfonso, A.; Li, M.; Cordova, M.; et al. In vivo tumor immune microenvironment phenotypes correlate with inflammation and vasculature to predict immunotherapy response. *Nat. Commun.* **2022**, *13*, 5312. [CrossRef]
88. Curiel-Lewandrowski, C.; Stratton, D.B.; Gong, C.; Kang, D. Preliminary imaging of skin lesions with near-infrared, portable, confocal microscopy. *J. Am. Acad. Dermatol.* **2021**, *85*, 1624–1625. [CrossRef]
89. Freeman, E.E.; Semeere, A.; Laker-Oketta, M.; Namaganda, P.; Osman, H.; Lukande, R.; McMahon, D.; Seth, D.; Oyesiku, L.; Tearney, G.J.; et al. Feasibility and implementation of portable confocal microscopy for point-of-care diagnosis of cutaneous lesions in a low-resource setting. *J. Am. Acad. Dermatol.* **2021**, *84*, 499–502. [CrossRef]
90. Larson, B.; Abeytunge, S.; Rajadhyaksha, M. Performance of full-pupil line-scanning reflectance confocal microscopy in human skin and oral mucosa in vivo. *Biomed. Opt. Express* **2011**, *2*, 2055–2067. [CrossRef]
91. Freeman, E.; Semeere, A.; Osman, H.; Peterson, G.; Rajadhyaksha, M.; González, S.; Martin, J.N.; Anderson, R.R.; Tearney, G.J.; Kang, D. Smartphone confocal microscopy for imaging cellular structures in human skin in vivo. *Biomed. Opt. Express* **2018**, *9*, 1906–1915. [CrossRef]
92. Gong, C.; Stratton, D.B.; Curiel-Lewandrowski, C.N.; Kang, D. Speckle-free, near-infrared portable confocal microscope. *Appl. Opt.* **2020**, *59*, G41–G46. [CrossRef] [PubMed]
93. Yelamos, O.; Cordova, M.; Peterson, G.; Pulitzer, M.; Singh, B.; Rajadhyaksha, M.; DeFazio, J. In vivo intraoral reflectance confocal microscopy of an amalgam tattoo. *Dermatol. Pract. Concept.* **2017**, *7*, 13–16. [CrossRef] [PubMed]
94. Peterson, G.; Zanoni, D.K.; Ardigo, M.; Migliacci, J.C.; Patel, S.G.; Rajadhyaksha, M. Feasibility of a Video-Mosaicking Approach to Extend the Field-of-View For Reflectance Confocal Microscopy in the Oral Cavity *In Vivo*. *Lasers Surg. Med.* **2019**, *51*, 439–451. [CrossRef] [PubMed]
95. Bianchetti, G.; Taralli, S.; Vaccaro, M.; Indovina, L.; Mattoli, M.; Capotosti, A.; Scolozzi, V.; Calcagni, M.; Giordano, A.; De Spirito, M.; et al. Automated detection and classification of tumor histotypes on dynamic PET imaging data through machine-learning driven voxel classification. *Comput. Biol. Med.* **2022**, *145*, 105423. [CrossRef]
96. Combalia, M.; Garcia, S.; Malvehy, J.; Puig, S.; Mülberger, A.G.; Browning, J.; Garcet, S.; Krueger, J.G.; Lish, S.R.; Lax, R.; et al. Deep learning automated pathology in ex vivo microscopy. *Biomed. Opt. Express* **2021**, *12*, 3103–3116. [CrossRef]
97. Sendín-Martín, M.; Lara-Caro, M.; Harris, U.; Moronta, M.; Rossi, A.; Lee, E.; Chen, C.-S.J.; Nehal, K.; Sánchez, J.C.-M.; Pereyra-Rodríguez, J.-J.; et al. Classification of Basal Cell Carcinoma in Ex Vivo Confocal Microscopy Images from Freshly Excised Tissues Using a Deep Learning Algorithm. *J. Investig. Dermatol.* **2022**, *142*, 1291–1299.e2. [CrossRef]
98. Wodzinski, M.; Skalski, A.; Witkowski, A.; Pellacani, G.; Ludzik, J. Convolutional Neural Network Approach to Classify Skin Lesions Using Reflectance Confocal Microscopy. In Proceedings of the 2019 41st Annual International Conference of the IEEE Engineering in Medicine and Biology Society, Berlin, Germany, 23–27 July 2019; Volume 2019, pp. 4754–4757. [CrossRef]
99. Campanella, G.; Navarrete-Dechent, C.; Liopyris, K.; Monnier, J.; Aleissa, S.; Minhas, B.; Scope, A.; Longo, C.; Guitera, P.; Pellacani, G.; et al. Deep Learning for Basal Cell Carcinoma Detection for Reflectance Confocal Microscopy. *J. Investig. Dermatol.* **2021**, *142*, 97–103. [CrossRef]
100. Soenen, A.; Vourc'H, M.; Dréno, B.; Chiavérini, C.; Alkhalifah, A.; Dessomme, B.K.; Roussel, K.; Chambon, S.; Debarbieux, S.; Monnier, J.; et al. Diagnosis of congenital pigmented macules in infants with reflectance confocal microscopy and machine learning. *J. Am. Acad. Dermatol.* **2021**, *85*, 1308–1309. [CrossRef]
101. Kose, K.; Bozkurt, A.; Alessi-Fox, C.; Gill, M.; Longo, C.; Pellacani, G.; Dy, J.G.; Brooks, D.H.; Rajadhyaksha, M. Segmentation of cellular patterns in confocal images of melanocytic lesions in vivo via a multiscale encoder-decoder network (MED-Net). *Med. Image Anal.* **2021**, *67*, 101841. [CrossRef]
102. Li, J.; Garfinkel, J.; Zhang, X.; Di Wu, D.; Zhang, Y.; de Haan, K.; Wang, H.; Liu, T.; Bai, B.; Rivenson, Y.; et al. Biopsy-free in vivo virtual histology of skin using deep learning. *Light. Sci. Appl.* **2021**, *10*, 233. [CrossRef]
103. Malciu, A.M.; Lupu, M.; Voiculescu, V.M. Artificial Intelligence-Based Approaches to Reflectance Confocal Microscopy Image Analysis in Dermatology. *J. Clin. Med.* **2022**, *11*, 429. [CrossRef]
104. Kose, K.; Bozkurt, A.; Alessi-Fox, C.; Brooks, D.H.; Dy, J.G.; Rajadhyaksha, M.; Gill, M. Utilizing Machine Learning for Image Quality Assessment for Reflectance Confocal Microscopy. *J. Investig. Dermatol.* **2020**, *140*, 1214–1222. [CrossRef]
105. Zhao, J.; Jain, M.; Harris, U.G.; Kose, K.; Curiel-Lewandrowski, C.; Kang, D. Deep Learning-Based Denoising in High-Speed Portable Reflectance Confocal Microscopy. *Lasers Surg. Med.* **2021**, *53*, 880–891. [CrossRef] [PubMed]
106. Ruini, C.; Schlingmann, S.; Jonke, Ž.; Avci, P.; Padrón-Laso, V.; Neumeier, F.; Koveshazi, I.; Ikeliani, I.U.; Patzer, K.; Kunrad, E.; et al. Machine Learning Based Prediction of Squamous Cell Carcinoma in Ex Vivo Confocal Laser Scanning Microscopy. *Cancers* **2021**, *13*, 5522. [CrossRef] [PubMed]
107. Sendín-Martín, M.; Kose, K.; Harris, U.; Rossi, A.; Lee, E.; Nehal, K.; Rajadhyaksha, M.; Jain, M. Complete visualization of epidermal margin during ex vivo confocal microscopy of excised tissue with 3-dimensional mosaicking and intensity projection. *J. Am. Acad. Dermatol.* **2022**, *86*, e13–e14. [CrossRef]
108. Cowen, E.A.; Sun, M.D.; Gu, L.; Acevedo, C.; Rotemberg, V.; Halpern, A.C. Store-and-forward mobile application as an accessible method of study participant assessment. *J. Eur. Acad. Dermatol. Venereol.* **2022**. [CrossRef] [PubMed]

109. Scope, A.; Dusza, S.; Pellacani, G.; Gill, M.; Gonzalez, S.; Marchetti, M.; Rabinovitz, H.; Marghoob, A.; Alessi-Fox, C.; Halpern, A. Accuracy of tele-consultation on management decisions of lesions suspect for melanoma using reflectance confocal microscopy as a stand-alone diagnostic tool. *J. Eur. Acad. Dermatol. Venereol.* **2018**, *33*, 439–446. [CrossRef]
110. Rubinstein, G.; Garfinkel, J.; Jain, M. Live, remote control of an in vivo reflectance confocal microscope for diagnosis of basal cell carcinoma at the bedside of a patient 2500 miles away: A novel tele-reflectance confocal microscope approach. *J. Am. Acad. Dermatol.* **2019**, *81*, e41–e42. [CrossRef]
111. Witkowski, A.; Łudzik, J.; Soyer, H.P. Telediagnosis with Confocal Microscopy: A Reality or a Dream? *Dermatol. Clin.* **2016**, *34*, 505–512. [CrossRef]